JOURNAL OF VIROLOGY, Oct. 1996, p. 6642–6652
0022-538X/96/$04.00+0

Vol. 70, No. 10

Autogenous Regulation of RNA Translation and Packaging by Rous Sarcoma Virus Pr76^{gag}

TAD S. SONSTEGARD[1]† AND PERRY B. HACKETT[1,2]*

Department of Genetics and Cell Biology, University of Minnesota, St. Paul, Minnesota 55108-1095,[1] and Institute of Human Genetics, University of Minnesota, Minneapolis, Minnesota 55455[2]

Received 7 December 1995/Accepted 14 June 1996

Unspliced cytoplasmic retroviral RNA in chronically infected cells either is encapsidated by Gag proteins in the manufacture of virus or is used to direct synthesis of Gag proteins. Several models have been suggested to explain the sorting of viral RNA for these two purposes. Here we present evidence supporting a simple biochemical mechanism that accounts for the routing of retroviral RNA. Our results indicate that ribosomes compete with the Gag proteins to determine the fate of nascent retroviral RNA. Although the integrity of the entire Rous sarcoma virus leader sequence is important for retroviral packaging and translation, the RNA structure around the third small open reading frame, which neighbors the Ψ site required for packaging of the RNA, is particularly critical for maintenance of the balance between translation and packaging. These results support the hypothesis that Gag proteins autogenously regulate their synthesis and encapsidation of retroviral RNA and that an equilibrium exists between RNA destined for translation and packaging that is based on the intracellular levels of Gag proteins and ribosomes. To test the model, mRNAs with natural or mutated 5′ leader sequences from Rous sarcoma virus were expressed in avian cells in the presence and absence of Pr76^{gag}. We demonstrate that Pr76^{gag} acts as a translational repressor of these mRNAs in a dose-dependent manner, supporting the hypothesis that Pr76^{gag} can sort retroviral RNA for translation and encapsidation.

Unspliced retroviral RNA is used either for synthesis of Gag proteins or for encapsidation to form infectious retrovirus. In avian sarcoma and leukosis viruses (ASLVs), ribosomes negotiate the RNA leader sequence to synthesize the precursor proteins Pr76^{gag} and Pr180$^{gag/pol}$, which in turn bind to the viral RNA, presumably at the encapsidation region designated Ψ which is contained within the leader (3, 14, 25–27, 32, 33, 35, 44). A balanced regulation of these two processes, mediated by the leader RNA sequence, is necessary for efficient viral propagation (8, 11, 12, 39).

Gag proteins serve two distinct functions in the propagation of retroviruses. They aid in the infection of host cells, and they direct assembly of viral particles in the infected cell. For assembly of infectious viral particles, Gag precursor must recognize and encapsidate two copies of unspliced viral RNA. Mutational studies of Gag polyproteins from murine leukemia virus, human immunodeficiency virus type 1 (HIV-1) and ASLVs have shown that a single sequence motif, composed of a cysteine array within the NC domain of the Gag polyprotein, is essential for recognition of viral RNAs during assembly (3, 4, 7a, 13, 17, 37, 38, 49, 51). The NC protein has been shown to bind in a specific manner to its RNA in HIV (3, 4, 7a, 14, 36, 50) and form particle-like structures with its cognate RNA (6).

In addition to requiring the NC domain of the Gag precursor for packaging, *cis*-acting signals on the viral RNA must be presented for recognition by Gag. One required encapsidation signal is Ψ, located within the 5′ leader sequences of all genomic retroviral RNAs (25, 33). The leader RNAs of ASLVs have a highly conserved RNA secondary structure, and both replication and packaging utilize the conserved structural motifs within the leader (18). The tRNA primer binding loop and a stem-loop structure (O3) important for encapsidation of the viral RNA, contained within the Ψ region of Rous sarcoma virus (RSV), have been partially confirmed by genetic and physical analyses, respectively (7, 27). In addition to conservation of secondary structure, the leaders of ASLV RNA contain the additional complexity of three open reading frames (ORF1, ORF2, and ORF3) which are phylogenetically conserved in size and position (18). The conservation of secondary structure and upstream ORFs within the ASLV leaders suggests that these elements are important in the life cycle of the virus (19).

Ribosome binding (9, 45–47) and translational studies in vitro (19, 23, 53) and in vivo (11, 12, 41, 42, 47) indicate that leader ORF1, ORF2, and possibly ORF3 are translated and that ribosomes move linearly from the cap site to the *gag* initiation codon. The effects of mutations in the ORFs on downstream translation were relatively minor in comparison with the effects on propagation of the retrovirus (41, 42), suggesting that translation of one or more of the ORFs is necessary for propagation of RSV. Specifically, mutations of the highly conserved sequence within ORF3 attenuate viral activities by altering the sequence and/or formation of the Ψ structure recognized for encapsidation of the RNA (9, 10, 33).

In some studies, the processes of translation and packaging appear to be functionally linked (11, 12, 41) in either of two ways, which we have named the direct coupling model and the indirect coupling model (Fig. 1A). In the direct coupling model, translation of ORF3 is required to shift the RNA secondary structure to a form recognizable for packaging (11). In the indirect coupling model, ORF3 encodes a peptide cofactor required for packaging (12). Both the direct and the indirect coupling models predict that an increase in the relative translational initiation strength at the initiation codon of ORF3, AUG3, will presumably increase the rate of Ψ formation and the availability of high-affinity binding sites for Gag to the viral

* Corresponding author. Mailing address: Department of Genetics and Cell Biology, University of Minnesota, 250 Biological Sciences, 1445 Gortner Ave., St. Paul, MN 55108-1095. Phone: (612) 624-6736. Fax: (612) 625-5754. Electronic mail address: perry@biosci.cbs.umn.edu.

† Present address: Roman L. Hruska Meat Animal Research Center, U.S. Department of Agriculture, Clay Center, NE 68933.

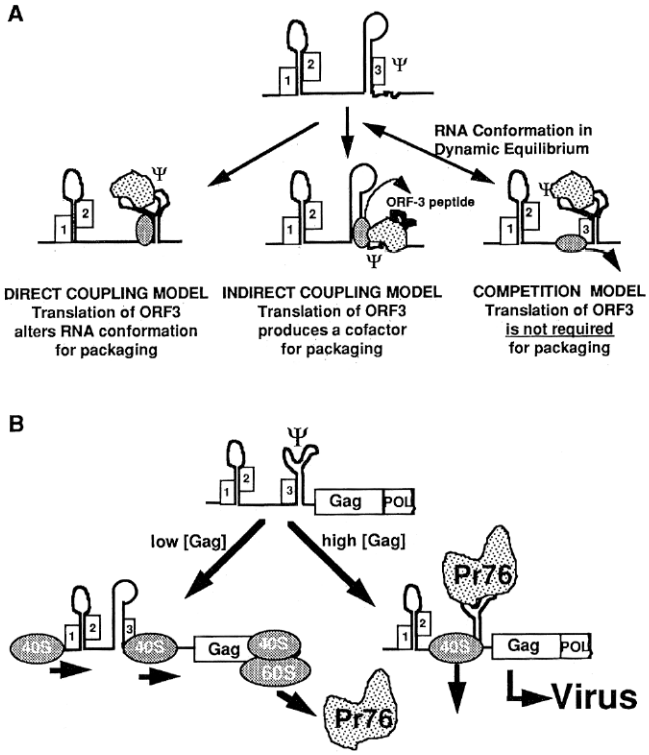

FIG. 1. Models for translation and packaging of RSV RNA. (A) The three models tested in this study. The models are described fully in the text. The three short ORFs in the 5′ leader sequence are shown by boxes. ORF3 is a part of the Ψ region that is required for packaging of retroviral RNA. In the direct coupling model and the competition model, the RNA structure around ORF3 and the Ψ region is represented as being able to adopt more than one conformation. The small arrow at the bottom of the competition model represents release of the ribosome (represented as shaded ovals) from RNAs bound by Gag (stippled structures) proteins. (B) Elaboration of the competition model shown in panel A showing the sorting of RNAs for either translation or encapsidation by Gag proteins. At low Gag (stippled proteins labeled Pr76) concentrations, nascent RNA emerging from the nucleus is most likely bound by ribosomal subunits (shaded ovals) which scan the leader, translate the small leader ORFs, and go on to translate the Gag cistron to produce Pr76^{gag} and Pr180$^{gag/pol}$. At high concentrations of Gag protein, there is a high probability that Gag molecules will bind to Ψ before the scanning subunit arrives to ORF3, thereby initiating selection of the viral RNA for encapsidation. The ribosomal subunit, unable to continue scanning, is released either before or after translation of ORF3.

RNA. An alternative model is that which we call the competition model (Fig. 1A), in which packaging and translation are in competition for nascent unspliced viral RNA. In this model, packaging is mediated by binding of Gag or Gag-Pol proteins to the Ψ site on RNA leader sequences that have not been traversed by scanning subunits, whereas translation depends on scanning of the leader RNA sequence by 40S ribosomal subunits, unhampered by bound Gag proteins (Fig. 1B); alternative structures in the Ψ region may form as a result of either ribosome passage or Gag binding. A mechanism similar to the competition model has been demonstrated for human hepatitis B virus and yeast LA virus, wherein modulation of ribosome movement through the packaging structure of pregenomic mRNAs regulates encapsidation (10, 24, 43, 48). The competition model is consistent with the results of early studies with murine leukemia virus, which indicated that the division of unspliced viral RNA into either a translational pool or a packaging pool occurred early after its synthesis (20) and that once RNA is associated with polysomes, it cannot be packaged (30, 31). The RNA sorting mechanisms have not been investigated for other retroviruses.

We took two approaches to determine the validity of these models of translation and packaging of RSV RNA. First, we tested the packaging and translation of model RNAs containing altered RSV leader sequences. Our results indicate that translation and packaging are not always functionally linked and that the sequence and/or structure of the entire RSV leader is important for optimal packaging and translation. Second, we tested one of the predictions of the competition model, that Gag protein is a repressor of translation of mRNAs containing Ψ regions in their leaders. The results from all of our experiments support the competition model for regulation of packaging and translation of retroviral RNA. Moreover, our findings suggest that the leader sequence of ASLV RNA is conserved to maintain a balance between translation and packaging of unspliced RNA and that decreasing either of these two processes by more than about 75% results in failure to produce virus.

MATERIALS AND METHODS

Cloning and mutagenesis. All plasmids were engineered by using standard techniques (52). Restriction enzymes, DNA-modifying enzymes, and DNA linkers were purchased from New England Biolabs and Gibco-BRL. Primers used in PCR, sequencing, and mutagenesis were synthesized by either National Bioscience, Inc., or Oligos Etc., Inc. PCR amplification of plasmid DNA was done in a Perkin-Elmer thermocycler. Mutagenesis was performed on uracil-rich single-stranded DNA isolated from *Escherichia coli* CJ236 (*dut ung* F′) (15). All plasmids were propagated in *E. coli* Top10F′ (Invitrogen) in the presence of 50 μg of ampicillin per ml. Plasmid integrity was verified by dideoxy sequencing. Plasmids used for riboprobe synthesis and transfection assays were purified with ion-exchange columns (Qiagen). All RSV cDNA was derived from the SR-A (SF) strain.

Cloning of pRL series plasmids. The mutant RSV 5′ leader sequences were cloned into the eukaryotic expression vector pGL2B (Promega), which contained the following features: (i) the entire promoter/U3 region from the SR-A (SF) strain of RSV, (ii) the RSV leader distal to the *gag* AUG, (iii) the first three amino acids of RSV *gag* fused to the fourth amino acid of the luciferase gene (*luc*), and (iv) the simian virus 40 (early) intron and poly(A) processing signal (Fig. 2A). To facilitate the fusion between the RSV *gag* leader and *luc* (RL), mutations were introduced into their respective coding regions by site-specific mutagenesis. First, pLTR-RI (47) and pUC118 were digested with *Hin*dIII and *Bam*HI. The 1,146-nucleotide (nt) RSV long terminal repeat fragment from pLTR-RI was ligated into the linearized phagemid to make pTLTR8. Mutagenesis was performed on pTLTR8 and pGL2B with the primers 5′-GCATGGAAGACGT CATTAAGG-3′ and 5′-GGCCTTTCTTTATGTTTTTGACGTCTTCC-3′, respectively, where the underlined base indicates the nucleotide change in each sequence to create *Aat*II restriction sites. The resultant plasmids, pTLTR8m and pGL2Bm, were digested with *Hin*dIII and *Aat*II. The 997-nt leader fragment from pTLTR8m was ligated into pGL2Bm to make pRLWT (WT, wild-type RSV leader). pRL-WT was subsequently used for the construction of all RSV leader plasmids that contained ORF mutations (Fig. 2A). For example, to introduce the AUG3 mutation into pRL-WT, pLTR-AUG3 and pRL-WT were digested with *Hin*dIII and *Sst*I, and the mutant RSV leader fragment from the former was replaced into the pRL-WT vector backbone. This plasmid was designated pRL-A3. A total of 11 ORF mutant leader constructs were cloned by using plasmid pRL7 (53).

Two primers were used to amplify DNA from plasmid pRL-WT to create a partial deletion of the O3 stem-loop structural element in the RSV leader sequence, 5′-TGTATCTTATGGTACTGTAACTG-3′ and 5′-CTAAGCCGC AGCCCCCTCC-3′. The amplified region spanned the entire RSV long terminal repeat and 5′ leader sequence proximal to the ORF3 termination. This PCR fragment was cloned into plasmid pRL-WT after digestion with *Sst*I, treatment with mung bean nuclease, and digestion with *Hin*dIII. For construction of pRL-SL, pLTR-AUG1 was digested with *Hin*dIII and *Sal*I, which cleaves at the site of the AUG1 mutation. This partial long terminal repeat fragment was filled in with Klenow enzyme, and the blunt ends were ligated into the *Sma*I-linearized pGL2B. To clone the 5′ hairpin (5′HP) element into the pRL series plasmids, pRL-WT was digested in two different reactions with *Cla*I and *Sst*I and with *Cla*I and *Eco*RI. From these reactions, 1,482-nt fragments corresponding to the 3′ end of the RSV leader fused to *luc* and the vector backbone fragment were isolated. pEHS-0.35 (47) was digested with *Hin*dIII to release a U3 fragment that was flush ended by using Klenow enzyme. The linear plasmid was digested with *Eco*RI, and a 51-nt fragment was isolated. pRSV-5′HP (23) was digested with *Sfc*I to release a 347-nt HP element, flush ended by using Klenow enzyme, and digested with *Sst*I. The HP fragment was ligated to the other three fragments in a single reaction.

Cloning of pRCG series plasmids. A series of RSV *gag* sequences were cloned into the eukaryotic expression plasmid pRC/CMV (Invitrogen) (Fig. 2B). These

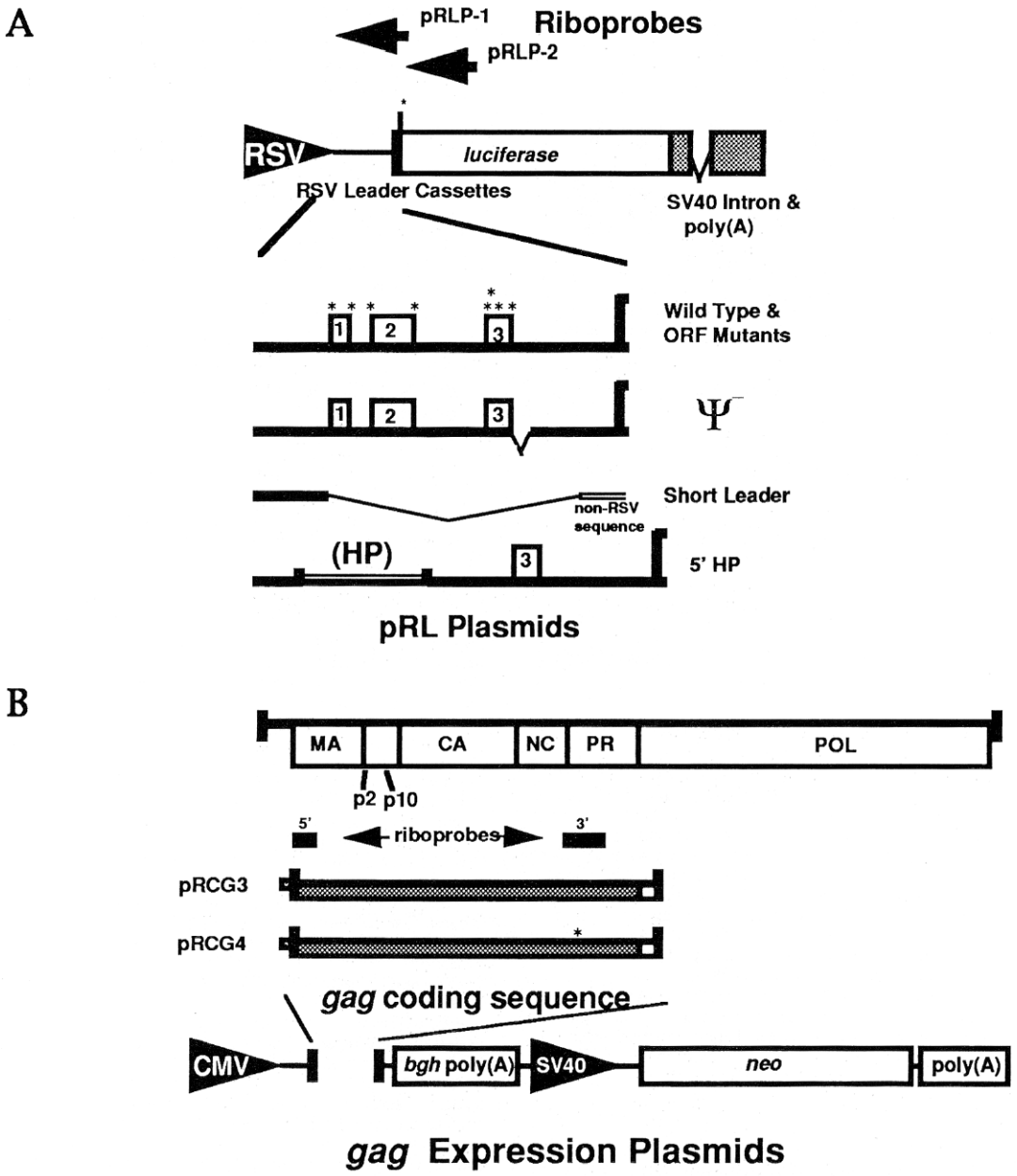

FIG. 2. Construction of pRL series plasmids and Gag expression vectors. (A) Schematic diagram of RSV leader-*luc* expression plasmids (pRL series) is shown at the top. The asterisk represents the mutation created to fuse the *gag* and *luc* coding sequences. The arrows labeled pRLP1 and pRLP2 represent antisense RNA fragments. The arrowhead represents the RSV SR-A1 promoter. The simian virus 40 (SV40) RNA processing signals are shown as filled boxes. The line between the RSV promoter and *luc* coding sequence represents the RSV 5′ leader cassette, which is expanded to show the sequences immediately upstream of *luc* in each construct. The four types of leader sequences are labeled to the right of each map. Single lines represent RSV leader sequence, and double lines are non-RSV-derived sequences. Breaks in the leader sequence lines represent deletions of sequence. The boxes on the black line represent ORFs. Distances are marked in nucleotides from the start of transcription. *, sites of mutagenesis to create mutations in either the ORFs or the RSV leader. (B) Top, map of the *gag* gene. The regions of *gag* mRNA protected with antisense *gag* riboprobes for RNase protection assays are shown below as dark bars labeled 5′ and 3′. The pRC constructs show the *gag* fragments inserted into plasmid pRC/CMV (bottom). The small square at the extreme left of the pRC inserts is a *Hin*dIII linker. *, restriction site created by site-specific mutagenesis. The arrowheads represent promoter and enhancer sequences. *bgh*, bovine growth hormone gene.

plasmids (pRCG) were constructed to express high levels of $Pr76^{gag}$ in *trans* to the RSV leader. pRCG plasmids contain the following features: (i) enhancer-promoter sequences from the immediate-early gene of human cytomegalovirus (CMV), (ii) a polylinker distal to the CMV promoter for insertion of RSV *gag*, (iii) polyadenylation signal and transcription termination sequences from the bovine growth hormone gene, and (iv) the *neo* gene, whose expression is regulated by the simian virus 40 promoter and poly(A) regions (Fig. 2B). A 2,470-bp fragment containing the RSV *gag* gene was cleaved from the infectious viral clone pSRA-1LTR (47) with *Sst*I and *Hpa*I and was cloned into pUC119. The plasmid, p9BH, was mutagenized, to introduce an *Nhe*I site 13 bp proximal to the initiation codon for $Pr76^{gag}$, with the primer 5′-TGGTCGGCTAGCGGATCA AGC-3′ . This clone, p9BH5′N, was digested with *Sst*I and *Eco*RI, and the 2,057-bp fragment was coligated with a 1,060-bp *gag/pol* gene fragment from *Eco*RI to *Xba*I into the *Sst*I and *Xba*I sites of pUC118. The resultant clone, p700G, was digested with *Nhe*I to release a 2,692-bp fragment, which was filled in with Klenow enzyme, and *Hin*dIII linkers were ligated onto the blunt ends. The linker ligation reaction was digested with *Hin*dIII, and the 2,374-bp fragment was ligated into pRC/CMV's *Hin*dIII polylinker site; the resulting construct was named pRCG3. For clone pRCG4, a *Bgl*II restriction site mutation (Asp-614→Arg) was introduced into the protease (PR) domain of *gag* (44). pRCβ-*gal*

was constructed by digestion of the *lacZ* gene with *Not*I. The 3.7-kb fragment was ligated into pRC/CMV at the *Not*I site.

Cloning of plasmids for in vitro transcription. pβactin2 (28) was digested with *Eco*RI and *Hin*dIII. The 4.7-kb fragment was isolated and ligated into the corresponding sites of the pBS(−) polylinker (Stratagene). This plasmid was designated pBS-β-actin. For construction of the *luc* riboprobe plasmids, pBS-WT-*luc* (53) was digested with *Hin*dIII, *Xba*I, and *Eco*RI to release two DNA fragments from the plasmid. These two fragments were ligated separately into the polylinker of pBS(−). pRLP1 contained the 423-nt fragment representing the *Hin*dIII-to-*Xba*I segment of the RSV leader-*luc* fusion, and pRLP2 contained the 540-nt fragment of the *luc* gene from *Xba*I to *Eco*RI. pBS-SBL was cloned by digestion of pSRA-1LTR with *Sst*I and *Bam*HI. The 269-bp fragment was cloned into the corresponding sites of pBS (Stratagene). This vector was used for synthesis of 5′ antisense riboprobes of *gag*. pBS-WT-*gag* was used to synthesize 3′ antisense riboprobes of *gag*.

In vitro synthesis of RNA. pBS-β-actin, pRLP1, and pRLP2 were linearized with *Nco*I, *Hin*dIII, and *Xba*I, respectively. Radiolabeled RNAs were synthesized from these linearized DNA templates with either 10 U of T3 or T7 RNA polymerase (Ambion) according to the manufacturer's protocol. After RNA synthesis, the DNA template was digested with 2 U of DNase I (Ambion) for 15 min at 37°C. Riboprobe specific activity was determined by trichloroacetic acid precipitation. The probe was either purified from the reaction mix with RNAid resin (Bio 101) or diluted directly into solution D (4 M guanidinium thiocyanate, 25 mM sodium citrate [pH 7], 0.5% [vol/vol] sarcosyl, 0.1 M 2-mercaptoethanol). Integrity of the probe was assessed by electrophoresis on a 5% (wt/vol) acrylamide–8 M urea gel.

Transfection. Cell lines were maintained as described previously (40, 55). Q2bn-4D and Qt6 cells were seeded at 0.5×10^6 cells per 60-mm-diameter plate. Following a 24-h incubation, the cells were transfected with a mix of pRL plasmid and helper plasmid DNA by a calcium phosphate method (2). All DNAs were diluted just prior to transfection. The transfection mix contained 10 μg of total DNA at either a 1:1 or 1:200 ratio of test to carrier plasmid; 6.9 ng of FV3*CAT* plasmid (5), which contains the *cat* gene driven by the carp β-actin promoter (34), was added to each mix to monitor transfection efficiencies by chloramphenicol acetyltransferase (CAT) assay (2). After a 12-h incubation, the transfection medium was removed. The cells were washed and replenished with 6 ml of fresh medium. Cells were incubated for 48 h posttransfection. For transient coexpression assays, the transfection mix was composed of 10 to 20 μg of DNA at selected ratios of pRCG to pRL plasmid DNA. The DNA plasmid mix for production of stable transformants contained 10 μg of total DNA at a 1:1 ratio of *gag* expression plasmid (pRCG3) to carrier plasmid DNA. Clonal cell lines were selected and propagated in DMEM medium supplemented with 200 μg of G418 per ml (2).

RNA packaging analysis of RSV leader mutations. For transfected Q2bn-4D cells, 6 ml of medium was collected from each 60-mm-diameter dish and replenished every 12 h over 48 h. Virions were harvested from the medium as described previously (1). After removal of the medium and buffer cushion, 100 μl of solution D was added to each tube. Virions were resuspended, and the lysed samples were collected and moved to a chilled Eppendorf tube.

RNase protection assays were performed as previously described (21), with slight modifications. A 40-μl portion of the sample was aliquoted into a RNA hybridization reaction tube. Each tube contained 2 to 8 fmol of a 546-nt antisense *luc* riboprobe and 1 fmol of a 311-nt antisense chicken β-actin riboprobe in 10 ml of solution D. The latter probe was added to monitor probe digestion conditions of each sample. The total amount of *luc* riboprobe added to each reaction was 1×10^5 to 2×10^5 cpm. Hybridizations were carried out for 16 h at 42°C. The samples were then digested in a 500 μl of RNase cocktail (10 mM Tris-HCl [pH 7.5], 300 mM NaCl, 5 mM EDTA, 500 U of RNase T_1, 10 μg of RNase A, 1.5 U of RNase H) for 1 h at 37°C. Control reactions of probe with and without digestion were also performed for each experiment to monitor assay conditions. After RNase digestion, 5 μl of proteinase K (20 μg/ml) and 20 μl of 10% (vol/vol) sarcosyl were added to each reaction tube. This reaction mix was incubated for 30 min at 37°C. Reaction products were precipitated with 500 μl of isopropyl alcohol containing 10 μg of *Torula* RNA per ml at −20°C for 30 min. The samples were then spun in a microcentrifuge at 10,000 × *g* for 15 min at 4°C. After careful aspiration, the pellets were air dried and then resuspended in 8 μl of loading buffer (80% [vol/vol] formamide, 0.1% [wt/vol] xylene cyanol, 0.1% [wt/vol] bromophenol blue, 2 mM EDTA). Samples were heated for 10 min at 75°C and then loaded onto a 0.75-mm-thick 8 M urea–5% (wt/vol) polyacrylamide gel. Gels were run at constant voltage of 250 V for 2 h. The gels were dried and exposed to X-ray film. RNA in each band of the gel was quantified by Phosphoimager (AMBIS) scan of the dried gel.

Virion samples were assayed for protein content by Western blotting (immunoblotting) (22), with slight modification. A 4-μl sample was diluted 1:5 in loading buffer (75 mM Tris-HCl [pH 6.8], 2% [vol/vol] sodium dodecyl sulfate [SDS], 10% [vol/vol] glycerol, 5% [vol/vol] 2-mercaptoethanol). After boiling, the virion samples and Pr-C virion protein standards were loaded and electrophoresed into a 0.75-mm-thick SDS–10% (wt/vol) polyacrylamide gel. Gels were blotted onto BA-S nitrocellulose (Schleicher & Schuell). The blots were washed, and viral proteins were hybridized to anti-RSV antibody diluted 1:5,000 (a gift from J. Wills). Viral protein-antibody complexes were detected after incubation to 6 μCi of ^{125}I-labeled goat anti-rabbit immunoglobulin G (12.9 μCi/μg; ICN Radiochemicals). Proteins in the blot were quantified by Phosphoimager (AMBIS) analysis. Blot integrity was monitored and confirmed by the Pr-C protein standard signals.

***luc* expression analysis of RSV leader mutants.** Plates of transfected cells were placed on ice, the medium was removed, and the cells were washed once with cold 1× phosphate-buffered saline (PBS). The cells were then collected into an Eppendorf tube by scraping in 1.5 ml of cold PBS and spun in a microcentrifuge at 2,000 × *g* for 5 min at 4°C. After aspiration, 1 ml of PBS was added to each tube, the cell pellet was gently resuspended and divided in half, and 500-μl aliquots were removed to new Eppendorf tubes. All samples were pelleted again, and the PBS was aspirated. For RNA analysis, one of the duplicate cell pellets was resuspended in 160 μl of solution D, mixed, and centrifuged for 1 min at 10,000 × *g*. A 40-μl aliquot was removed to an Eppendorf tube containing 10 μl of the riboprobe used for virion RNA analysis. For analysis of *gag* RNA, either a 269-nt anti-5′ or a 234-nt anti-3′ *gag* riboprobe was added to the riboprobe mix. The reactions were performed and analyzed in the same manner as for the RNase protection assays for virion RNA.

For protein analysis, the second 500-μl aliquot of cells was pelleted and resuspended in 400 μl of 1× lysis buffer (25 mM bicine [pH 7.6], 0.5% [vol/vol] Tween 20, 0.5% [vol/vol] Tween 80). The cells were mixed and incubated for 15 min at room temperature. The nuclei were pelleted for 2 min at 10,000 × *g* in a microcentrifuge. The supernatant was removed to a new tube, and samples were immediately assayed for Luc activity according to the manufacturer's protocol (Promega). To ensure that the assay conditions corresponded to the linear part of the response curve, pilot assays of serially diluted extracts were performed, and the results were compared with those of parallel assays with serial dilution of commercial, purified Luc (Boehringer Mannheim). Reactions were measured in a Lumat LB9501 luminometer (Berthold), and Luc activity was expressed as relative light units. Total protein concentration of cellular extract samples was determined by fluorometry (57). Generally, 7.5 μl of undiluted sample extract was added to 1.5 ml sodium Na borate (pH 9.5). Then 500 μl of 0.03% (wt/vol) fluorescamine in acetonitrile was mixed into each sample. Samples were incubated for 10 min at room temperature and assayed in a Spectra/glo filter fluorometer (Gilson). The millivolt output was converted to micrograms of protein by using a standard curve generated by measurement of bovine serum albumin diluted in 1× lysis buffer.

RESULTS

Translation and packaging of RL mRNAs. We constructed a series of 15 plasmids with mutations in the RSV leader fused to the *luc* reporter gene to determine the interdependency of translation and packaging (Fig. 2A). The RL RNAs, synthesized from an RSV promoter, encoded a luciferase protein that had four amino-terminal residues from Pr76^{gag}. We examined the effects of the RSV leader mutations on translation and packaging of RL RNAs following transfection of either Qt6 or Q2bn-4D quail cells with the DNA constructs. The Qt6 cells were used to test the translational efficiencies of the RL mRNAs in the absence of viral proteins. The Q2bn-4D cells were used to test both the translational and packaging efficiencies of the RL RNAs in the presence of a constant level of viral packaging proteins (1, 55), without the additional complexity of altered viral protein synthesis from mRNAs which contain mutations in the leader ORFs (12).

Our strategy for expression and packaging analysis of the RL RNAs is diagrammed in Fig. 3. Effects on translation of the mutations in the ORFs were quantified by using assays of *luc* gene expression following isolation of extracts from each plate of transfected cells. To ensure that the enzymatic activities of Luc reflected translational efficiencies rather than differential transcription from the constructs, the levels of cellular RL mRNAs were determined by RNase protection. Packaged RL RNA levels were similarly determined from virion samples isolated from the extracellular media of transfected Q2bn-4D cells. Figure 4A shows that WT, 5′HP, and A1 RNAs were efficiently encapsidated. 5′HP mRNA contains a 162-nt inverted repeat which forms an 81-bp stem-loop 17 nt from the 5′ cap site and represses translation of the mRNA in vitro, presumably by inhibition of ribosome scanning (23). Conversely short leader (SL), Ψ^-, A3, and FS3TC3 RNAs were not encapsidated efficiently. SL RNAs contained only the first 41 nt of the RSV leader connected to 29 nt of plasmid se-

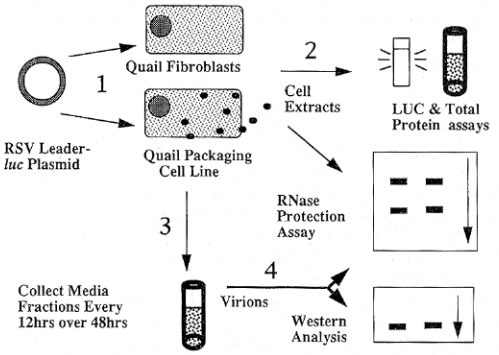

FIG. 3. Strategy for examining packaging and translation of RSV leader model RNAs. 1, RSV leader-*luc* constructs are transfected into quail cells for analysis of transient expression; 2, the upper pathway represents assays of cellular extracts to determine translational efficiencies and cellular levels of steady-state mRNAs; 3, the lower vertical arrow represents the collection of media and isolation of virions from transfected Q2bn-4D cells; 4, the lower horizontal pathway represents assays to determine efficiencies of RNA packaging.

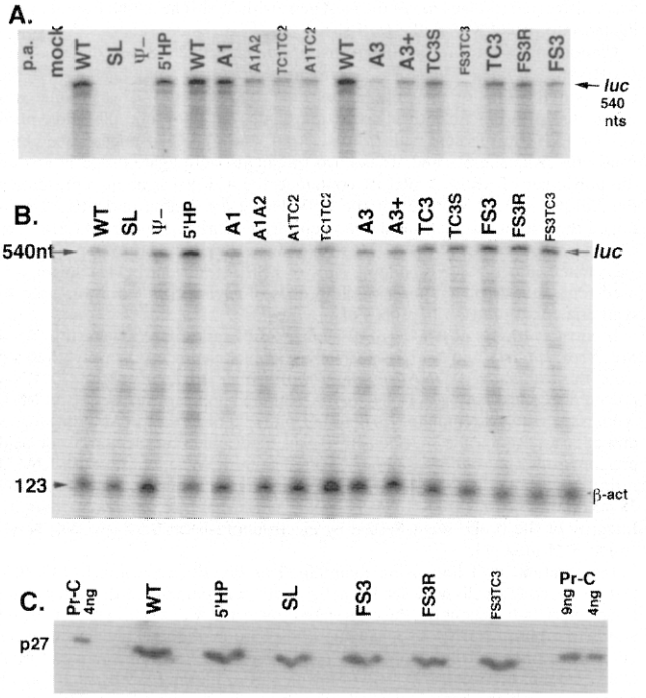

FIG. 4. Analysis of virion and cellular RNAs and proteins by RNase protection and Western assays. RNA analysis by RNase protection assay of virion (A) and cellular (B) RL mRNAs. Hybridizations and digestions were done as stated in Materials and Methods. (A) RNase-digested samples were electrophoresed through 5% polyacrylamide–urea gels for resolution of protected bands. The RNA leader types are indicated above the lanes; designations represent ORF mutations (e.g., A1 is a mutation in the AUG codon of ORF1, and TC1 is a mutation of the termination codon of ORF1). Virions were harvested at 12, 24, 36, and 48 h from Q2bn-4D cells transfected with 5 μg of pRL plasmid and 5 μg of carrier DNA. A 40-μl fraction of each isolate was hybridized to the 546-nt pRLP2 antisense riboprobe. The 540-nt protected fragment corresponds to sequences within *luc*. Mock, RNA assayed from virions isolated from Q2bn-4D cells transfected with carrier plasmid DNA; p.a. (probe alone), a sample of probe hybridized and digested without cell extract. (B) Sample lanes represent one-eighth equivalent of extract from a 60-mm-diameter plate of transfected Q2bn-4D cells. The 123-nt band corresponds to the second exon of β-actin mRNA protected after hybridization to a 311-nt antisense riboprobe transcribed from the chicken β-actin gene. (C) Autoradiogram of Western analysis used to determine CA levels in virions harvested from extracellular media of transfected Q2Bn-4D cells. Lanes are marked as in panels A and B. CA was detected as described in Materials and Methods. Protein standards are labeled for amount of total viral protein loaded per lane on both sides of the gel.

quence upstream of the *luc* AUG. This RNA contained neither the RSV ORFs nor the RSV Ψ element in its leader. Ψ⁻ RNAs contained a deletion which removed the sequences involved in formation of the 3′ stem portion of the O3 structural element in Ψ (18, 27). The other RNAs were encapsidated at intermediate levels. The amount of SL mRNA was about 40% below that of WT mRNA in the cell, suggesting a rapid turnover (Fig. 4B), while 5′HP mRNA was exceptional in that it was present in high amounts in both virions and cells, indicating that it more stabile than WT mRNA. The intracellular levels of the other RL mRNAs were relatively constant and varied less than twofold from the WT RNA level between assays. Virion protein levels were determined by Western analysis (Fig. 4C), and the values obtained were used to control for differences in virions between samples as described below for calculation of packaging efficiency. These results showed that RL RNAs were differentially translated and packaged, while virus particle production was stable.

Data similar to those shown in Fig. 4 were used to calculate the following four parameters for each mRNA: (i) cellular mRNA levels, calculated as ^{32}P cpm of *luc* mRNA/^{32}P cpm of β-actin mRNA; (ii) translational efficiency, calculated as Luc enzymatic activity (relative light units)/(microgram of cellular protein/cellular mRNA level); (iii) packaging efficiency, calculated as ^{32}P cpm of *luc* virion RNA/^{125}I cpm of virion protein CA; and (iv) selectivity of packaging, calculated as packaging efficiency/cellular mRNA level, where the latter three values for each mutant RL mRNA were normalized to the value for RSV WT RNA. For example, for 5′HP mRNA, translational efficiency (5′HP) equals translational efficiency (5′HP)/translational efficiency (WT), packaging efficiency (5′HP) equals packaging efficiency (5′HP)/packaging efficiency (WT), and selectivity of packaging (5′HP) equals selectivity of packaging (5′HP)/selectivity of packaging (WT). Each of the parameters was determined a minimum of four times in each cell line unless indicated otherwise.

Decoupling of translation and packaging. The translational and packaging efficiencies of RNAs expressed from plasmids pRL-SL, pRL-Ψ⁻, and pRL-5′HP were measured to determine if the processes of RSV leader translation and packaging could be dissociated (Fig. 5A). SL and Ψ⁻ mRNAs had slightly enhanced translational efficiencies in comparison with WT mRNA, whereas packaging of these RNAs was about an order of magnitude lower than that of WT RNAs, equivalent to the background level of this assay. These results support the idea that the Ψ region, which includes portions of the O3 stem-loop structure, is required for efficient packaging of viral RNA. pRL-5′HP was constructed to test the effects of inhibition of ribosome movement through the RSV leader on translation and packaging. The translational efficiency of 5′HP mRNA was reduced 10- to 20-fold, a repression that is nearly equal to that found in vitro (23, 53). In contrast, the packaging efficiency of 5′HP RNA was only 25% below that of WT RNA, which demonstrates that the Ψ element was able to initiate packaging in the absence of normal ribosome movement through the RSV leader. However, because the cellular levels of 5′HP mRNA were also higher than that of WT RNA (Fig. 4B), there was actually a two- to threefold decrease in the selectivity of packaging of 5′HP RNA (Fig. 5A). The results of assays using Ψ⁻ and 5′HP mRNAs clearly contradict the direct and indirect coupling models, which hypothesize that ribosome movement through the RSV Ψ region is required for encapsidation of RSV RNA.

	Leader Type	Translational Efficiency: Qt6 Cells	Translational Efficiency: Q2bn Cells	Packaging: Efficiency	Packaging: Selectivity
A	WT	1.00	1.00	1.00	1.00
	SL	1.74±.35	1.39±.23	0.11±.02	0.17±.03
	Ψ-	1.10±.26	1.25±.11	0.07±.01	0.07±.01
	5'HP	0.03±.02	0.08±.02	0.78±.04	0.28±.02
B	WT	1.00	1.00	1.00	1.00
	A3	2.09±.05	1.36±.15	0.14±.02	0.13±.02
	A3+	0.71±.01	0.94±.05	0.26±.03	0.24±.02
	TC3S	0.53±.04	1.30±.10	0.58±.06	0.51±.06
	FS3 TC3	0.30±.04	0.71±.06	0.16±.02	0.11±.02
	FS3	0.12±.03	0.23±.07	0.27±.03	0.25±.04
	FS3R	0.29±.05	0.63±.07	0.73±.12	0.67±.08
	TC3	0.59±.05	0.79±.07	0.68±.13	0.64±.14

FIG. 5. Influence of the RSV leader on translation and packaging of model RNAs. Each construct is shown on the left, using the same symbols as in Fig. 1. The values to the right represent the translational efficiency and RNA packaging activity of each RL RNA normalized to WT RNA levels and are mean values from at least four independent experiments ± standard errors. Each independent experiment always included pRL-WT for reference. (A) RL mRNAs with major alterations in the 5′ leader sequence. (B) Influence of ORF3 on translation and packaging of model RNAs. Horizontal stripes in the ORF3 mutants indicate the −1 reading frame and vertical stripes indicate the +1 reading frame relative to the AUG codon of ORF3.

Mutations in ORF3 repress encapsidation. Previous studies of RSV leader ORF1 and ORF2 demonstrated that alteration of their AUGs delayed viral spread, suggesting that the leader sequence is important for both translation and packaging of viral RNAs (11, 12, 41, 42, 47). Accordingly, we examined the association between packaging and translation in four ORF mutants with deletions or extensions of ORF1 and ORF2 which had delayed viral phenotypes (41, 47). We found there was a correlation of translational efficiencies with packaging efficiencies (53), indicating that these regions are important for both processes. In contrast, previous phenotypic analyses of ORF3 mutants demonstrated that efficient propagation of RSV was sensitive to changes in the initiation context and length of ORF3 (11, 12, 41). These observations suggested that an increase in ribosome movement through ORF3 and the Ψ region abrogated packaging. Alternatively, mutations within ORF3 might have affected the ability of the O3 RNA structural motif to form and/or be recognized by Pr76^{gag} (or Pr180$^{gag/pol}$) for packaging (for example, see reference 41). We tested eight ORF3 mutations in this study to distinguish between the two possibilities (Fig. 4 and 5). The results presented in Fig. 5B show that alteration of the initiation codon of ORF3 (A3) enhanced the translational efficiency of A3 mRNA in both Qt6 and Q2bn-4D cells, although the efficiencies were slightly reduced in the presence of viral proteins. The packaging efficiency of the A3 RNA was approximately seven- to eightfold lower than that of WT RNA, similar to the packaging efficiency of the SL and Ψ$^-$ RNAs (Fig. 4A and Fig. 5A). Thus, the translational efficiency of A3 RNA was more than an order of magnitude greater than its packaging efficiency. These results agree with the hypothesis either that ribosomal recognition of AUG3 is necessary for encapsidation (direct and indirect coupling models) or that the mutation of the O3 stem-loop perturbs the formation of an RNA structure and its recognition by Gag proteins required to initiate packaging (competition model).

To distinguish between the models, other mutations in ORF3 which change the AUG3 initiation context and/or ORF3 length were tested for translation and packaging. Changing the +4 nt of AUG3 from an A to a G, to put the AUG codon in an optimal context (A3$^+$), slightly reduced downstream translation of *luc* but repressed RNA packaging efficiencies fourfold (Fig. 4A and 5A). The effects on translation and packaging of A3$^+$ RNA were not correlated, suggesting that the reduced packaging of the A3 RNA is a result of alteration of the O3 structure, in agreement with the competition model. The TC3S and FS3TC3 mutations each elongate ORF3 from 9 to 26 amino acids by a frameshift mutation, but the FS3TC3 mutant retains the same AUG codon initiation context as the AUG3$^+$ mutant. In Q2bn-4D cells, translational repression was reduced for FS3TC3 mRNA, while the translational efficiency of the TC3S mRNA was 30% greater than that of WT mRNA. This result suggests that the mutations in TC3S facilitate ribosome movement downstream to the *gag* initiation codon in the presence of viral protein. The packaging efficiency and selectivity of TC3S RNA was repressed 40 to 50%, while packaging of FS3TC3 RNA was repressed to near background levels.

Mutant RSV leader sequences FS3, FS3R, and TC3 extend ORF3 from 9 to 64 amino acids, thereby causing ORF3 to overlap the *luc* coding sequence by 22 nt. FS3 RNA was repressed about fourfold in both translational and packaging efficiency compared with WT RNAs. The RNAs that were mutated only by extension of ORF3 (FS3R and TC3) were repressed about 20 to 40% in translational efficiency and about 30 to 40% in packaging efficiency. The packaging of RL mRNAs A3$^+$, FS3TC3, and FS3 RNAs, all of which have an AUG codon context that increases initiation of translation at AUG3 (53), was low, which is inconsistent with the direct coupling model for translation and packaging. The data are consistent with the hypothesis that mutation of the +4 nt of ORF3 represses encapsidation of the RNA either by alteration of the O3 structure in Ψ or by increasing translational initiation at AUG3, which in turn negatively regulates packaging. The variable levels of packaging for RNAs with altered ORF3 sequences contradict the indirect coupling model, in which the encoded peptide plays a role. In contrast, the parallel changes in translation and packaging are consistent with a competition between translation and packaging that is dependent on the integrity of the O3 substructure of Ψ, which is influenced by some but not all mutations in ORF3. For unknown reasons, the translation efficiencies of all of the ORF3 mutant mRNAs were greater in Q2bn-4D cells than in Qt6 cells.

Qtg cells expressing Pr76^{gag} repress translation of model RNAs with an RSV leader sequence. If the competition model is correct, then Gag should be a translational repressor and increasing the ratio of Gag protein to RL mRNAs with intact Ψ elements should lower the translational efficiencies of the mRNAs. We used two strategies to determine whether Pr76^{gag} could autoregulate downstream translation of model RNA

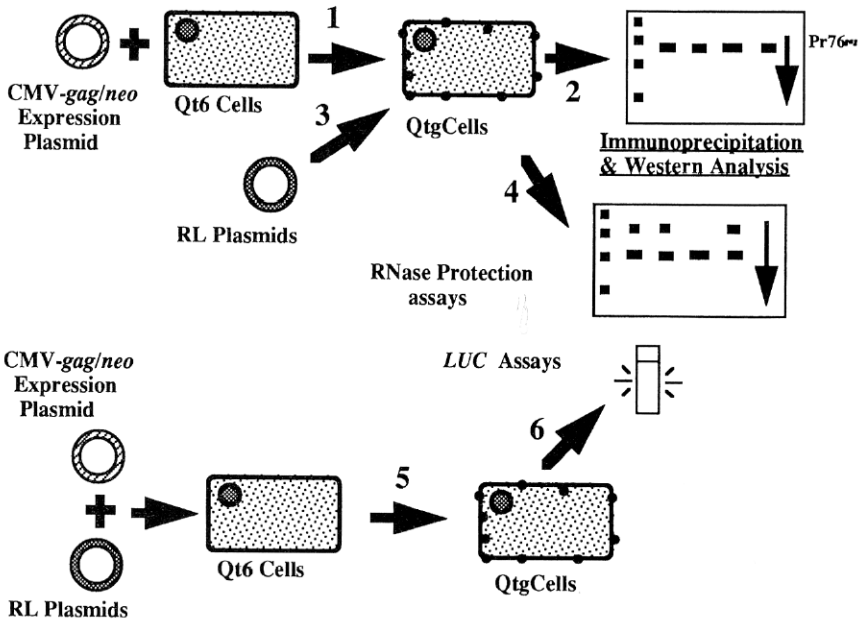

FIG. 6. Strategies for analysis of Pr76^{gag} regulation of translation. Steps 1 to 4, transfection of CMV-*gag* plasmids (striped ring) into quail Qt6 cells (step 1) to produce stable clonal cell lines that express RSV Gag protein (Qtg cells with dots representing Gag protein molecules). *gag* expression from cellular extracts of Qtg cell lines to determine steady-state levels of Gag protein was measured (step 2). Gag-expressing cells were transfected (step 3) with RL plasmids (filled ring), which encode Luc behind a complete RSV 5′ leader sequence, and the translational efficiencies of RL mRNAs were determined by calculating the ratio of Luc protein (*LUC* Assays) to RL mRNA (RNase Protection assays) as shown in step 4. Alternatively, CMV-*gag* plasmids and RL plasmids were cotransfected together into Qt6 cells (step 5). RL plus *gag* mRNA production and the translational efficiencies of RL mRNAs were quantified (step 6).

with a RSV leader sequence. First, as shown in steps 1 to 4 in Fig. 6, we measured the translational efficiencies of the RL mRNAs in two different Qtg avian cell lines which constitutively expressed Pr76^{gag} as a result of prior transformation with CMV-*gag* constructs (the pRCG constructs shown in Fig. 2B). Second, as shown in steps 5 and 6 in Fig. 6, we cotransfected avian cells with pRL reporter plasmids plus Pr76^{gag} expression plasmids and measured the effects of transiently expressed Gag on the translational efficiency of the RL mRNA. The pRCG expression clones were constructed by deleting most of the leader cap proximal to the *gag* AUG, to eliminate binding of Pr76^{gag} to the *gag* mRNAs and the consequential autoregulation of Gag expression. The 5′ leader sequence in the pRCG constructs is nearly optimal for initiation of translation (29), 56 nt from the transcriptional start site in pRCG3 and 46 nt in the other *gag* expression vectors shown in Fig. 2B.

To study translational regulation by the polyprotein, we constructed two Qtg cell lines, 37.2 and 37.5, that had relatively high rates of expression of *gag* mRNA and Pr76^{gag}. Neither of these lines produced unusual Gag-related polypeptides that might have interfered with our analyses. Qtg line 37.5 expressed the highest level of unspliced *gag* mRNA, about 500 copies of full-length *gag* mRNA per cell, as determined from an estimate of 10,000 copies of β-actin mRNA per cell and the specific activities of the respective riboprobes. Pr76^{gag} protein was detected by immunoprecipitation and Western blotting in all of the Qtg lines that expressed *gag* mRNA (53).

Our Gag autoregulation model predicts that Pr76^{gag} is a translational inhibitor of mRNAs containing the Ψ packaging site in their leader sequences and that as the ratio of Pr76^{gag} to the mRNA decreases, the translational efficiency of the mRNA will increase. Accordingly, we cotransfected low concentrations of pRL-WT, which has the complete RSV RNA leader sequence preceding the *luc* gene (Fig. 2A), and a CAT expression construct (pFV3*CAT*) into the Qtg cell lines. Sample transfections were assayed in duplicate for each experiment; transfection of the Qtg line 16.4, which does not express Gag protein, was used as the negative control. Luc activity was normalized to total protein and CAT activity to normalize transfectional efficiency. Translational efficiencies of the RL mRNAs in the presence of Pr76^{gag} were calculated as follows: translational efficiency$_{RL\ mRNA}$ = Luc activity (+Gag cell line)/Luc activity(−Gag cell line).

The results of these experiments are shown in Fig. 7. Translation of RL mRNAs was inhibited in both the cell lines at about the same rate. At the highest Gag-to-RL mRNA ratio,

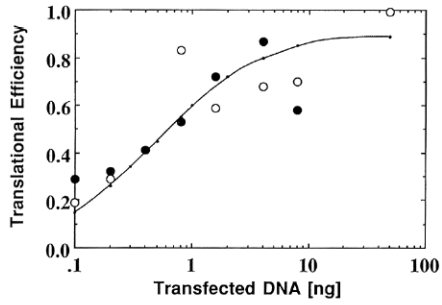

FIG. 7. Translational analysis of RL RNA in Qtg cell lines. Cellular extracts from Qtg 37.2 and 37.5 cells transfected with plasmid pRL-WT were assayed for Luc activity, CAT activity, and total protein. Translational efficiencies were calculated as described in the text. The translational efficiencies of the −Gag samples were assayed from transfection extracts of the non-*gag*-expressing cell line 16.4 that was transformed with pRC/CMV. The average translational efficiencies (*y* axis) from three independent experiments, each of which was conducted with duplicate samples, were determined and plotted against the amounts of transfected test plasmid (*x* axis). Open circles, Qtg cells 37.2; filled circles, Qtg cells 37.5. The theoretical curve, translational efficiency$_{RL\ mRNA}$ = 0.9[pRL-WT]/([pRL-WT] + 0.5), described in the text, is shown by the line through the small points, with $K = 0.9$ and $C = 0.5$ (arbitrary units).

corresponding to the lowest level of transfected pRL-WT, the translational efficiency was reduced 70 to 80%. Increased concentrations of transfected pRL-WT resulted in a reduction in the inhibition of *luc* translation. Inhibition was almost completely relieved when 50 ng or more of pRL-WT was transfected. Kinetically, the reaction of RL mRNA with either Gag or ribosomes can be modeled. Assuming that the RL mRNAs are in competition with other cellular mRNAs for ribosomes and/or translational initiation factors, the translational efficiency of RL-mRNA can be described as follows: translational efficiency$_{RL\ mRNA}$ = K[pRL-WT]/([pRL-WT] + C), where C and K are association constants of Gag and ribosomes to RL mRNA and the cellular concentrations of ribosomes and Gag protein, respectively. None of these values are known, but they should be about the same in Qtg 37.2 and 37.5 cells lines since the Gag protein concentrations in these cell lines were about the same. As shown in Fig. 7, the data could be fitted to the equation after the values for K and C were derived by substituting experimental values into the equation and solving for the two constants. In this equation, which describes the situation wherein the Gag protein concentration is constant but the input RL mRNA concentration varies, the value of K is the highest attainable translational efficiency. In our particular experiments, the best solution resulted in a K value of about 0.9, indicating that at high pRL-WT input (>5 ng), when most of the model mRNA is translated, ribosome binding dominates over Gag binding, presumably because of the relatively low level of Gag protein in the Qtg cells. More detailed biochemical measurements are required to determine precise association constants of Gag with the RL mRNAs. Although the data do not prove that Gag operates as a simple repressor of translation, they are consistent with this hypothesis. More importantly, these results demonstrate that the effect of Gag on translation of RL mRNAs is dose dependent.

Translational efficiencies of RSV-*luc* RNA in avian cells cotransfected with *gag* expression plasmids. To circumvent the problem of low Gag output by the Qtg cell lines, we used the second strategy shown in Fig. 6 to measure translational efficiencies over a wider concentration range of Pr76^{gag}. In these experiments, we cotransfected normal quail Qt6 cells with pRL-WT plus either pRCG3 (which encodes Pr76^{gag}) and pRCG4 (which encodes a protease-deficient mutant of Pr76^{gag}). The translational efficiencies for the RL mRNAs were determined in the same manner as the transfections into the Qtg cell lines. The results shown in Fig. 8 demonstrate that as the molar ratio of either pRCG plasmid to pRL-WT plasmid DNA was increased, the translational efficiency of RL mRNA decreased. The reduction in translational efficiencies of RL mRNAs saturated at a *gag* DNA-to-RL DNA molar ratio of about 20,000:1; 80% repression of translation was obtained in the presence of WT Pr76^{gag}. Although both WT and PR$^-$ forms of Gag acted as translational inhibitors, for unknown reasons there was a slight difference in repressive effects between the two types of Pr76^{gag} at high Gag levels.

The kinetics of inhibition in Fig. 7 and 8 are expected to differ; in Fig. 8, the concentration of RL mRNA was essentially constant and the Gag concentration varied, whereas in Fig. 7, the RL mRNA concentration varied and the Gag concentration was constant. If the Qt6 cells took up the same ratio of *gag* and RL DNAs as were provided for transfection, then the following equation should be valid: translational efficiency$_{RL\ mRNA}$ = 1/(1 + Q[Gag]), where Q is proportional to the association constant of Gag to RL mRNA and the relative transfectional efficiencies of the input plasmids. In Fig. 8, where [Gag] is expressed in terms of the input ratio of pRCG to pRL-WT, a best fit for the equation occurs with Q equal to 1.5×10^{-4}.

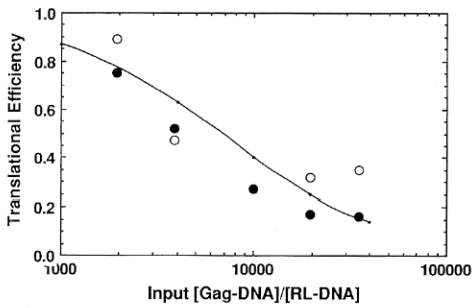

FIG. 8. Translational analysis of RL RNA coexpressed with *gag*. Cellular extracts from Qt6 cells cotransfected with *gag* expression plasmids and plasmid pRL-WT were assayed for Luc activity, CAT activity, and total protein. Translational efficiencies were calculated as described in Results. The translational efficiencies of −Gag samples were assayed from extracts cotransfected with pRCβ-*gal*. The average values from three or more independent experiments were determined and plotted against the ratio of CMV-*gag* to pRL-WT plasmid transfected. Filled circles, pRCG3 (WT Gag); open circles, pRCG4 (PR$^-$ Gag). The theoretical curve, with a best-fit value when Q equals 1.5×10^{-4}, is shown by the line through the small points: translational efficiency$_{RL\ mRNA}$ = 1/(1+ 1.5×10^{-4}[Gag]).

Even in these experiments in which we could control the ratio of Gag to RL mRNA, two constraints prohibited us from achieving complete repression of RL mRNA translation. First, the large number of ribosomes (estimated to be about 5×10^6 per cell in tissue culture) ensures that some RL mRNA will be bound by ribosomes. Second, some cells will be transfected only by RL DNA without accompanying *gag* DNA; these cells will translate RL mRNA in an unrestricted manner. Regardless of this limitation, these results qualitatively support the conclusion derived from the Qtg transfection results, that Gag inhibits translation of RL mRNA in a dose-dependent manner.

Our model predicts that the repression of translation should result from Gag binding to the putative Gag-binding Ψ region in the RSV RNA leader sequence. Accordingly, we evaluated the ability of Gag to repress translation of two mutant RL mRNAs, Ψ$^-$, which has a deletion of most of the Ψ sequence, and SL, which lacks nearly all of RSV leader sequence, including the Ψ element (Fig. 2A). These RNAs are packaged about 10-fold less efficiently than WT-*luc* RNAs (Fig. 5A). In contrast to the inhibition of translation of WT RNA, translation of Ψ$^-$ mRNA was not repressed even at high levels of Gag. SL mRNA was resistant as expected at intermediate levels of Gag (53). These results demonstrate that translation of RL mRNAs that contain the Ψ sequence are repressed by Gag proteins in a dose-dependent manner, whereas those that lack a Ψ region are not.

DISCUSSION

In this study, we used model RL RNAs to examine the relationship between translation of the ORFs in the 5′ leader sequence of RSV and packaging of RSV leader RNA. As shown most dramatically in Fig. 5A, packaging of RL RNAs was not dependent on translation of the RSV 5′ leader RNA. 5′HP RNA, whose leader contained a functional RSV Ψ element accompanied by a translational block near the 5′ cap site, was packaged at approximately 75% of the rate of WT RNA (Fig. 4A and 5). The packaging efficiency of 5′HP RNA strongly suggests that ribosome movement through the leader is not necessary for packaging of the RNA, thereby supporting the competition model but not the coupling models (Fig. 1).

Our results are in accord with previous findings with murine leukemia virus that suggested RNA that was routed to either a pool for translation or a pool for packaging and that RNA bound by ribosomes could not be packaged (30, 31). The necessity of the O3 stem-loop structure for packaging of RSV RNAs was demonstrated by the Ψ^- and SL mutant RNAs. These two RNAs were not able to form the functional O3 structural element of the Ψ element and, as predicted by the competition model, were packaged at minimal rates.

The role of the ORFs in packaging of RSV RNA has been exhaustively examined by us and others, and different conclusions have been suggested. Reconciliation of the translational differences between our model RNAs shown here and those of Donzé et al. (11, 12) is a bit difficult because of variations in sequence alterations that perturb RNA secondary structure, the methods used to quantify packaging and translation, and the use of two different strains of RSV. The most important difference in our results centers around the role of ORF3. We suggest that the ORF is translated minimally and that its translation is of minor consequence to encapsidation, whereas Donzé et al. concluded that translation of ORF3 is important to encapsidation. A presumably important experiment was to measure the translation of ORF3 by insertion of the *luc* gene behind ORF3. However, ORF3 is in a particularly unstable region of RNA secondary structure (18) such that insertion of the gene alters local RNA secondary structure, which could alter translational initiation at AUG3. Thus, the use of *luc* as a reporter for ORF activity by us (53) and others (11, 12) cannot fully resolve the extent to which an ORF is translationally active. In any case, the key to interpreting all of the available data is to separate mutations in ORF3 that affect the ORF as a distinct entity from those that affect the folding of the RNA in the ORF3 and Ψ regions. When this is done, all of the published data can be consistently interpreted as supporting the hypothesis that RNA secondary structure is more important for packaging than for translation of the RNA sequence around Ψ. For example, if either ribosome stalling (12) or ORF3 translation (11) enhances encapsidation of RSV leader RNA, then the $A3^+$ RNA should package more efficiently than WT RNA. Our results show that it does not. The packaging results for $A3^+$ RNA parallel those of 5′HP RNA (Fig. 5), suggesting that perturbations of the O3 stem-loop motif in Ψ have effects on packaging that depend on the sites of the mutations (41). Alteration of the AUG codon and the bases that immediately follow it in ORF3 can affect the structure of the O3 stem-loop (54). The importance of these specific bases is supported by phylogenetic analysis which demonstrates the conservation of RNA structure rather than sequence among all examined strains of ASLV (18).

Mechanistic aspects of translational regulation by Pr76^{gag}. Our results show that translation of RL mRNAs which contained the wild-type RSV 5′ leader sequence was repressed by Pr76^{gag} in a dose-dependent manner. This translational repression by Pr76^{gag} appears to saturate at a molar ratio of Gag protein to RSV RNA of at least 2,000:1 when the appropriate packaging motifs are contained within the RSV 5′ leader RNA. Although the amount of Gag protein in the Qtg cell lines was low, the translational efficiencies of RL mRNAs were repressed. When Ψ, a region genetically implicated in packaging, was absent from the RL mRNA leaders, translation was not repressed in a dose-dependent manner. These results are consistent with an autoregulatory mechanism in which Pr76^{gag} routes viral RNA into pools for translation and packaging.

The foregoing results strongly suggest that Gag should bind to Ψ. However, we have been unable to show a direct physical interaction between Pr76^{gag} and the RSV leader RNA (53). Though disappointing, our inability to show a direct interaction between Pr76^{gag} and RSV 5′ leader was not surprising because although many groups have tried to detect Gag binding to retroviral Ψ regions, in the type C retroviruses, only HIV-1 Gag precursor has been shown to bind its own RNA specifically (3, 14, 35, 36). The lack of Gag binding to limited regions of the RSV RNA leader harboring Ψ (sequences less than 200 nt) suggests that Ψ is necessary, but not sufficient, for stable association of Gag molecules to the RNA (53).

Our results do not address specifically the type of Gag-RNA interaction that inhibits translation. We envision that the interaction could be of two sorts. Either Pr76^{gag} binds to the RNA and sterically interferes with ribosome scanning or Pr76^{gag} binds to the RNA to form a ribonucleoprotein complex that precludes ribosome binding to the 5′ end of the RNA. If the Ψ element is a nucleation site of Pr76^{gag} binding to RNA, a single Pr76^{gag}-RSV RNA complex may not be sufficient to inhibit downstream translation. Studies done on translational regulation of ferritin mRNAs show that a single protein-RNA binding complex inhibits downstream translation only when placed within 40 nt of the 5′ cap of the mRNA (16); the 5′ boundary of the Ψ structural element is 159 nt from the cap (25). The data in Fig. 7 and 8 are not sufficiently precise to predict the number of Gag proteins required for repression. However, we surmise that in the chronically infected cell, cooperative binding of hundreds of Gag proteins occurs once an RNA binds one or more initial Gag proteins at a site such as Ψ. Once encapsidated, the nascent core particle containing 2,000 to 3,000 Gag proteins is exported from the cell (56), thereby raising the chances that nascent RSV RNA will be recognized by ribosomes before being bound by Gag protein.

The balance between translation and packaging of retroviral RNA is critical for virus spread. Obviously the ability of a retrovirus to replicate requires both translation and encapsidation of the viral RNA, but to what degree can these two processes be unbalanced yet support viral replication? To address this question, we plotted the translational and packaging properties of the model RSV RNAs as a function of the corresponding effects that the mutations have on viral replication (Fig. 9) as determined in previous experiments (41, 42). Minimal efficiencies of packaging and translation needed for retroviral propagation can be inferred from the plots in Fig. 9. Mutations which are outside the Ψ region retard the rates of virus spread (Fig. 9A). The slowing of propagation of the mutant viruses correlates with the reductions in translational and packaging efficiencies of their RNAs. For example, A1 RNA is slightly inhibited in translation and packaging (41, 42), and the onset of viral propagation is delayed a few days (47), while the double mutants, A1A2 and TC1TC2, have reduced packaging and translation, and their replication is delayed twice as long as that of the A1 virus (41).

Mutations which lie within sequences of the O3 structural element in Ψ result in either wild-type or attenuated phenotypes (Fig. 9B). All of the live viruses (FS3R, TC3, and TC3S) have mutations in ORF3 that are not in the AUG codon or codon context region (41, 53). The levels of repression of translational efficiencies vary in these mutant RNAs, but all package at a rate 50% of that of WT RNA. In contrast, mutations that abolish the AUG3 codon (A3) or improve its translational context ($A3^+$, FS3, and FS3TC3) lower packaging rates below 25% of the WT RNA rate and prevent spread of the virus in our assay system (47). These observations suggest that a threshold level of packaging, approximately 25% of the WT RNA level, is necessary for propagation of RSV. In addition, viral protein translation must be maintained above 30% to maintain RSV propagation (41).

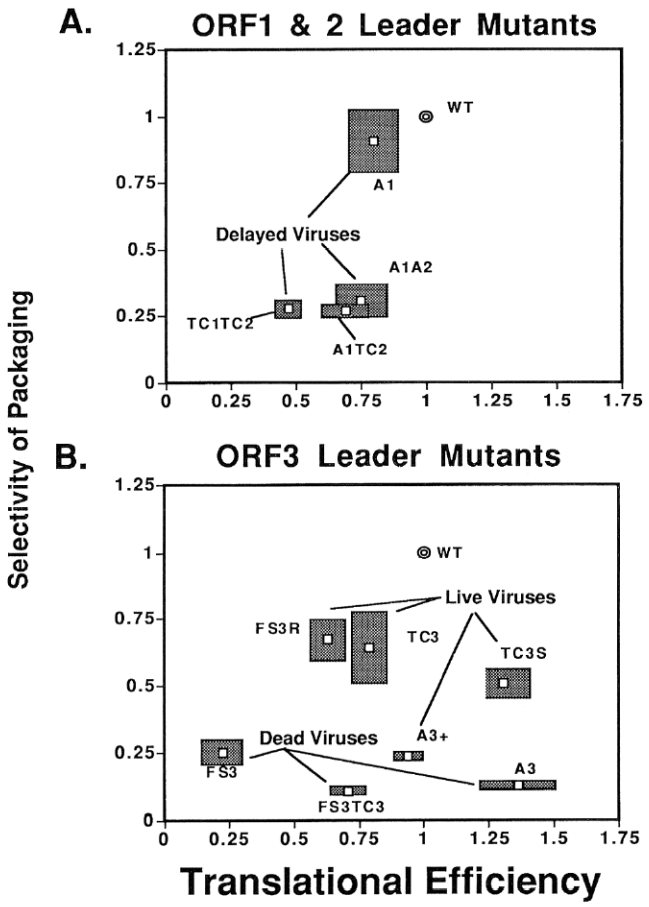

FIG. 9. Relationships between translation and packaging of RSV model retroviral RNAs to viral phenotype. Relationships between translation and packaging of RSV RNAs and viral phenotype. Plots of results shown in Fig. 5 are shown. *x* axis, translational efficiency; *y* axis, selectivity of packaging of the RL mRNAs. The shaded regions represent the standard error values of the average ranges. Viral phenotypes of previously characterized mutants (41, 42, 53) are labeled and identified by lines to their corresponding mutant RSV model RNA values, and WT is represented as a double ring for reference.

In summary, the packaging and translational efficiencies of the mutant RSV RNAs described in this study suggest that the ORFs have been conserved to regulate scanning through the RSV leader. Analyses of mutations within ORF3 suggest that this sequence is conserved for Pr76^{gag} (or Pr180$^{gag/pol}$) recognition of the Ψ motif in O3 and that its length is conserved to allow for efficient downstream translation. The overlap of conserved sequence motifs for translation and packaging of unspliced retroviral RNAs maintains the balance between these two processes, which is mediated by a translational product of the *gag* gene. What then is the purpose(s) of the conserved ORFs in the 5′ leader sequences of all ASLVs? It appears from our results on packaging and those of others who have studied reverse transcription (7) that distinct structural motifs in the RNA are required for two retroviral activities, binding of reverse transcriptase and binding of Gag proteins to the retroviral RNA. The ORFs appear to facilitate the third activity of the RNA, templating protein synthesis. In the case of RSV, translation of the highly structured viral RNA is aided by the presence of ORFs which temporarily convert the scanning subunits to complete ribosomes which can better negotiate stable RNA conformations, as demonstrated in HIV (39). We hypothesize that the different retroviruses encode proteins that recognize specific RNA motifs, not all of which are refractory to scanning by ribosomal subunits. This conclusion suggests that the sorting mechanism mediated by Gag proteins described here is universal for all retroviruses whether they have 5′ leader ORFs or not.

ACKNOWLEDGMENTS

We thank L. Atac and M. Portlance for help in the construction and sequencing of some of the pRL plasmids, A. Faras for the gift of the Pr-C protein standards, John Wills for the gift of anti-RSV antibody, Maxine Linial for the gift of the Q2bn-4D cell line, and S. Fahrenkrug, J. Essner, A. Yeo, M. Stoltzfus, A. Moustakas, R. Petersen, and two reviewers for helpful insights, conversations, and suggestions to improve the manuscript.

This work was supported by grants from the American Cancer Society (IN/NP-790) and the University of Minnesota Leukemia Task Force.

REFERENCES

1. **Aronoff, R., and M. Linial.** 1991. Specificity of retroviral RNA packaging. J. Virol. **65:**71–80.
2. **Ausubel, F. M., R. Brent, R. E. Kingston, D. D. Moore, J. A. Smith, J. G. Seidman, and K. Struhl (ed.).** 1987. Current protocols in molecular biology. John Wiley & Sons, New York.
3. **Berkowitz, R. D., J. Luban, and S. P. Goff.** 1993. Specific binding of human immunodeficiency virus type 1 *gag* polyprotein and nucleocapsid protein to viral RNAs detected by RNA mobility shift assays. J. Virol. **67:**7190–7200.
4. **Berkowitz, R. D., A. Ohagen, S. Hoglund, and S. P. Goff.** 1995. Retroviral nucleocapsid domains mediate the specific recognition of genomic viral RNAs by chimeric Gag polyproteins during RNA packaging. J. Virol. **69:**6445–6456.
5. **Caldovic, L., and P. B. Hackett.** 1995. Development of position-independent expression vectors and their transfer into transgenic fish. Mol. Mar. Biol. Biotechnol. **4:**51–61.
6. **Campbell, S., and V. M. Vogt.** 1995. Self-assembly in vitro of purified CA-NC proteins from Rous sarcoma virus and human immunodeficiency virus type 1. J. Virol. **69:**6487–6497.
7. **Cobrinik, D., L. Soskey, and J. Leis.** 1988. A retroviral RNA secondary structure required for efficient initiation of reverse transcription. J. Virol. **62:**3622–3630.

7a. **Dannull, J., A. Surovoy, G. Jung, and K. Moelling.** 1994. Specific binding of HIV-1 nucleocapsid protein to PSI RNA in vitro requires N-terminal zinc finger and flanking basic amino acid residues. EMBO J. **13:**1525–1533.

8. **Darlix, J.-L.** 1986. Control of Rous sarcoma virus RNA translation and packaging by the 5′ and 3′ untranslated sequences. J. Mol. Biol. **189:**421–434.
9. **Darlix, J.-L., P.-F. Spahr, P. A. Bromley, and J.-C. Jaton.** 1979. In vitro, the major ribosome binding site on Rous sarcoma virus RNA does not contain the nucleotide sequence coding for the N-terminal amino acids of the *gag* gene product. J. Virol. **29:**597–611.
10. **Dinman, J. D., and R. B. Wickner.** 1992. Ribosomal frameshifting efficiency and *gag/gag-pol* ratio are critical for yeast M1 double-stranded RNA virus propagation. J. Virol. **66:**3669–3676.
11. **Donzé, O., P. Damay, and P.-F. Spahr.** 1995. The first and third uORFs in RSV leader RNA are efficiently translated: implications for translational regulation and viral RNA packaging. Nucleic Acids Res. **23:**861–868.
12. **Donzé, O., and P.-F. Spahr.** 1992. Role of the open reading frames of Rous sarcoma virus leader RNA in translation and genome packaging. EMBO J. **11:**3747–3757.
13. **Dupraz, P., and P.-F. Spahr.** 1992. Specificity of Rous sarcoma virus nucleocapsid protein in genomic RNA packaging. J. Virol. **66:**4662–4670.
14. **Geigenmuller, U., and M. L. Linial.** 1990. Specific binding of human immunodeficiency virus type 1 (HIV-1) Gag-derived proteins to a 5′ HIV-1 genomic RNA sequence. J. Virol. **70:**667–671.
15. **Geisselsoder, J., F. Witney, and P. Yuckenberg.** 1987. Efficient site-directed *in vitro* mutagenesis. Bio Technology **5:**786–791.
16. **Goossen, B., and M. W. Hentze.** 1992. Position is the critical determinant for function of iron-responsive elements as translational regulators. Mol. Cell. Biol. **12:**1959–1966.
17. **Gorelick, R. J., L. E. Henderson, J. P. Hanser, and A. Rein.** 1988. Point mutants of Moloney murine leukemia virus that fail to package viral RNA: evidence for specific RNA recognition by a "zinc finger-like" protein sequence. Proc. Natl. Acad. Sci. USA **85:**8420–8424.
18. **Hackett, P. B., D. P. Johnson, M. W. Dalton, and R. B. Petersen.** 1991. Phylogenetic and physical analysis of the 5′ leader RNA sequences of avian retroviruses. Nucleic Acids Res. **19:**6929–6934.
19. **Hackett, P. B., R. B. Petersen, C. H. Hensel, F. Alberico, S. I. Gunderson, A. C. Palmenberg, and G. Barany.** 1986. Synthesis *in vitro* of a seven amino acid peptide encoded in the leader RNA of Rous sarcoma virus. J. Mol. Biol. **190:**45–57.

20. **Hackett, P. B., H. E. Varmus, and J. M. Bishop.** 1981. The genesis of Rous sarcoma virus messenger RNAs. Virology **112:**714–728.
21. **Haines, D. S., and D. H. Gillespie.** 1992. RNA abundance measured by a lysate RNase protection assay. Bio/Technology **12:**736–741.
22. **Harlow, E., and D. Lane.** 1988. Antibodies: a laboratory manual. Cold Spring Harbor Laboratory, Cold Spring Harbor, N.Y.
23. **Hensel, C. H., R. B. Petersen, and P. B. Hackett.** 1989. Effects of alterations in the leader sequence of Rous sarcoma virus RNA on initiation of translation. J. Virol. **63:**4986–4990.
24. **Junker-Niepman, M., R. Bartenschlager, and H. Schaller.** 1990. A short *cis*-acting sequence is required for hepatitus B virus pregenome encapsidation and sufficient for packaging of foreign RNA. EMBO J. **9:**3389–3396.
25. **Katz, R. A., R. W. Terry, and A. M. Skalka.** 1986. A conserved *cis*-acting sequence in the 5′ leader of avian sarcoma virus RNA is required for packaging. J. Virol. **59:**163–167.
26. **Kawai, S., and T. F. Koyama.** 1984. Characterization of a Rous sarcoma virus mutant defective in packaging its own genomic RNA: biochemical properties of mutant TK15 and mutant-induced transformants. J. Virol. **51:**154–162.
27. **Knight, J. B., Z. H. Si, and C. M. Stoltzfus.** 1994. A base-paired structure in the avian sarcoma virus 5′ leader is required for efficient encapsidation of RNA. J. Virol. **68:**4493–4502.
28. **Kost, T. A., N. Theodorakis, and S. H. Hughes.** 1983. The nucleotide sequence of the chick cytoplasmic β-actin gene. Nucleic Acids Res. **11:**8287–8301.
29. **Kozak, M.** 1991. Effects of long 5′ leader sequences on initiation by eukaryotic ribosomes *in vitro*. Gene Expr. **1:**117–123.
30. **Levin, J. G., P. M. Grimley, J. M. Ramseur, and I. K. Berezsky.** 1974. Deficiency of 60 to 70S RNA in murine leukemia virus particles assembled in cells treated with actinomycin D. J. Virol. **14:**152–161.
31. **Levin, J. G., and M. J. Rosenak.** 1976. Synthesis of murine leukemia virus proteins associated with virions assembled in actinomycin-D-treated cells: evidence for persistence of viral messenger RNA. Proc. Natl. Acad. Sci. USA **73:**1154–1158.
32. **Linial, M., E. Medeiros, and W. S. Hayward.** 1978. An avian oncovirus mutant (*SE*21Q1b) deficient in genomic RNA: biological and biochemical characterization. Cell **15:**1371–1381.
33. **Linial, M., and A. D. Miller.** 1990. Retroviral RNA packaging: sequence requirements and implications. Curr. Top. Microbiol. **157:**125–152.
34. **Liu, Z., B. Moav, A. J. Faras, K. S. Guise, A. R. Kapuscinski, and P. B. Hackett.** 1990. Functional analysis of elements affecting expression of the β-actin gene of carp. Mol. Cell. Biol. **10:**3432–3440.
35. **Luban, J., and S. P. Goff.** 1991. Binding of human immunodeficiency virus type 1 (HIV-1) RNA to recombinant HIV-1 *gag* polyprotein. J. Virol. **65:**3203–3212.
36. **Luban, J., and S. P. Goff.** 1994. Mutational analysis of *cis*-acting packaging signals in human immunodeficiency virus type 1 RNA. J. Virol. **68:**3784–3793.
37. **Meric, C., and S. P. Goff.** 1989. Characterization of Moloney murine leukemia virus mutants with a single-amino-acid substitutions in the Cys-His box of the nucleocapsid protein. J. Virol. **63:**1558–1568.
38. **Meric, C., E. Gouilloud, and P.-F. Spahr.** 1988. Mutations in Rous sarcoma virus nucleocapsid protein p12 (NC): deletions of Cys-His boxes. J. Virol. **62:**3328–3333.
39. **Miele, G., A. Mouland, G. P. Harrison, E. Cohen, and A. M. L. Lever.** 1996. The human immunodeficiency virus type I 5′ packaging signal structure affects translation but does not function as an internal ribosomal entry site structure. J. Virol. **70:**944–951.
40. **Moscovici, C., M. G. Moscovici, H. Jimenez, M. C. M. Lai, M. J. Hayman, and P. K. Vogt.** 1977. Continuous tissue culture cell lines derived from chemically induced tumors of Japanese quail. Cell **11:**95–103.
41. **Moustakas, A., T. S. Sonstegard, and P. B. Hackett.** 1993. Alterations of the three short open reading frames in the Rous sarcoma virus leader RNA modulate viral replication and gene expression. J. Virol. **67:**4337–4349.
42. **Moustakas, A., T. S. Sonstegard, and P. B. Hackett.** 1993. Effects of the open reading frames in the Rous sarcoma virus leader RNA on translation. J. Virol. **67:**4350–4357.
43. **Nassal, M., M. Junker-Niepmann, and H. Schaller.** 1990. Translational inactivation of RNA function: discrimination against a subset of genomic transcripts during HBV nucleocapsid assembly. Cell **63:**1357–1363.
44. **Oertle, S., and P.-F. Spahr.** 1990. Role of the *gag* polyprotein precursor in packaging and maturation of Rous sarcoma virus genomic RNA. J. Virol. **64:**5757–5763.
45. **Petersen, R. B., and P. B. Hackett.** 1985. Characterization of ribosome binding on Rous sarcoma virus RNA in vitro. J. Virol. **56:**683–690.
46. **Petersen, R. B., C. H. Hensel, and P. B. Hackett.** 1984. Identification of a ribosome-binding site for a leader peptide encoded by Rous sarcoma virus RNA. J. Virol. **51:**722–729.
47. **Petersen, R. B., A. Moustakas, and P. B. Hackett.** 1989. A mutation in the short 5′-proximal open reading frame on Rous sarcoma virus RNA alters virus production. J. Virol. **63:**4787–4796.
48. **Pollack, J. R., and D. Ganem.** 1993. An RNA-stem-loop structure directs hepatitus B virus genomic RNA encapsidation. J. Virol. **67:**3254–3263.
49. **Rein, A., D. P. Harvin, J. Mirro, S. M. Ernst, and R. J. Gorelick.** 1994. Evidence that a central domain of nucleocapsid protein is required for RNA packaging in murine leukemia virus. J. Virol. **68:**6124–6129.
50. **Sakaguchi, K., N. Zambrano, E. T. Baldwin, B. A. Shapiro, J. W. Erickson, J. G. Omichinski, G. M. Clore, A. M. Gronenborn, and E. Appella.** 1993. Identification of a binding site for the human immunodeficiency virus type 1 nucleocapsid protein. Proc. Natl. Acad. Sci. USA **90:**5219–5223.
51. **Sakalian, M., J. W. Wills, and V. M. Vogt.** 1994. Efficiency and selectivity of RNA packaging by Rous sarcoma virus *gag* deletion mutants. J. Virol. **68:**5969–5981.
52. **Sambrook, J., E. F. Fritsch, and T. Maniatis.** 1989. Molecular cloning: a laboratory manual, 2nd ed. Cold Spring Harbor Laboratory, Cold Spring Harbor, N.Y.
53. **Sonstegard, T. S.** 1995. Roles of the Rous sarcoma virus 5′ leader RNA sequence and the $Pr76^{gag}$ protein in translation. Ph.D. thesis. University of Minnesota, St. Paul.
54. **Sonstegard, T. S.** Unpublished data.
55. **Stoker, A., and M. J. Bissel.** 1988. Development of avian sarcoma and leukosis virus-based vector-packaging cell lines. J. Virol. **62:**1008–1015.
56. **Vogt, V. M., R. Eisenman, and H. Diggelmann.** 1975. Generation of avian myeloblastosis virus structural proteins by proteolytic cleavage of a precursor polyprotein. J. Mol. Biol. **96:**471–493.
57. **Weigele, M., S. De Bernardo, J. Tengi, and W. Leimgruber.** 1972. A novel reagent for the fluorometric assay of primary amines. J. Am. Chem. Soc. **94:**5927.
58. **Witherall, G. W., J. M. Gott, and O. C. Uhlenbeck.** 1991. Specific interaction between RNA phage coat proteins and RNA. Prog. Nucleic Acid Res. Mol. Biol. **40:**185–219.